Developmental Cell, Vol. 2, 785–796, June, 2002, Copyright ©2002 by Cell Press

Do Morphogen Gradients Arise by Diffusion?

Arthur D. Lander,[1,3] Qing Nie,[2] and Frederic Y.M. Wan[2]
[1]Department of Developmental and Cell Biology
Developmental Biology Center
[2]Department of Mathematics
University of California, Irvine
Irvine, California 92697

Summary

Many patterns of cell and tissue organization are specified during development by gradients of morphogens, substances that assign different cell fates at different concentrations. Gradients form by morphogen transport from a localized site, but whether this occurs by simple diffusion or by more elaborate mechanisms is unclear. We attempt to resolve this controversy by analyzing recent data in ways that appropriately capture the complexity of systems in which transport, receptor interaction, endo- and exocytosis, and degradation occur together. We find that diffusive mechanisms of morphogen transport are much more plausible—and nondiffusive mechanisms much less plausible—than has generally been argued. Moreover, we show that a class of experiments, endocytic blockade, thought to effectively distinguish between diffusive and nondiffusive transport models actually fails to draw useful distinctions.

Introduction

From fly wings to frog embryos to chick limbs, tissue patterns appear to be specified by gradients of morphogens, among which are growth factors of the TGF-β, Wingless, and Hedgehog families (Briscoe and Ericson, 1999; McDowell and Gurdon, 1999; Nellen et al., 1996; Neumann and Cohen, 1997; Strigini and Cohen, 1997; Tickle, 1999; Zecca et al., 1996). That morphogens are indeed distributed in gradients has been established (Entchev et al., 2000; Strigini and Cohen, 2000; Teleman and Cohen, 2000), but how gradients arise is controversial (e.g., McDowell et al., 2001; Pfeiffer and Vincent, 1999). Arguments against morphogen movement by diffusion have been raised by many, including Kerszberg and Wolpert (1998) who asserted that capture of morphogens by receptors so impedes diffusion that useful stable gradients can never arise by that mechanism. They proposed that morphogens instead use a "bucket brigade" mechanism in which receptor-bound morphogen on one cell moves by being handed off to receptors on an adjacent cell.

Expression in *Drosophila* wing discs of the morphogen Dpp fused to green fluorescent protein (Dpp-GFP) has recently permitted visualization of a gradient as it forms in vivo (Entchev et al., 2000; Teleman and Cohen, 2000). Some observations in such discs seem at odds with diffusive tranpsort. For example, much labeled Dpp is found not around cells, but within them; blockade of endocytosis in responding cells causes defects in Dpp transport; and genetic ablation of receptors in small clones of cells results in accumulation of Dpp at the side of the clone facing the Dpp source. Such results have been taken as evidence for morphogen transport by transcytosis—the sequential endocytosis and exocytosis of bound ligands (Entchev et al., 2000). Indeed, the notion that Dpp and other morphogens, such as Wingless and Hedgehog, all move through tissues by transcytosis or similar processes is increasingly accepted by many (e.g., Greco et al., 2001; Moline et al., 1999; Narayanan and Ramaswami, 2001; Pfeiffer and Vincent, 1999), albeit not all (McDowell et al., 2001; Strigini and Cohen, 2000), investigators.

Has it been settled that diffusion does not create morphogen gradients? We assert that, on the contrary, when the data are correctly interpreted, they not only fail to rule out diffusive transport, they favor it. By carrying out an analysis of morphogen transport in which interacting dynamic processes (diffusion, binding, dissociation, internalization, etc.) are explicitly accounted for, we draw three conclusions.

First, useful morphogen gradients can form by diffusion in tissues that contain morphogen receptors, provided that receptor numbers, kinetics, and (critically) internalization and degradation meet conditions that, as it happens, fit well with observations. Second, the observed effects of endocytic blockade on morphogen transport do not imply that endocytosis must be part of the transport process. Third, to explain the establishment of known morphogen gradients by nondiffusive mechanisms (e.g. transcytosis or bucket brigades) certain cell biological processes would have to occur at implausibly fast rates.

Results

Dynamic systems, such as those involving molecular transport, often defy casual intuition and are best approached mathematically. When Kerszberg and Wolpert (1998) simulated morphogen diffusion over 180 receptor-bearing cells, they concluded that, if capture by receptors is efficient, morphogens will saturate all receptors in a region of tissue before diffusing further. Instead of a broad gradient of receptor activation, a "wave" of complete receptor activation would spread out from the morphogen source. From this analysis, they rejected the idea that in vivo gradients form by diffusion.

Here we take a different approach, numerically solving equations that govern morphogen movement and receptor binding. We focus on the *Drosophila* wing disc so that comparisons with recent measurements (Entchev et al., 2000; Teleman and Cohen, 2000) can be made.

Receptors Impede, but Do Not Preclude, Gradient Formation

For the purpose of calculation, we simplify the geometry of a wing disc to a one-dimensional diffusion problem

[3]Correspondence: adlander@uci.edu

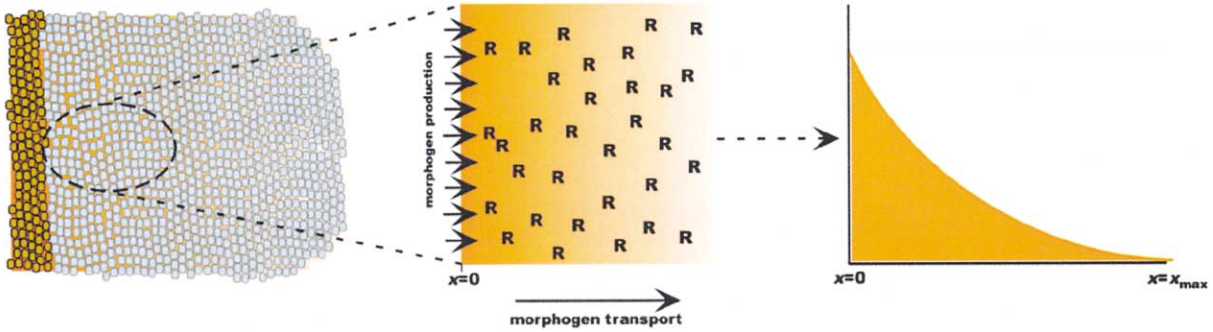

Figure 1. Views of a Morphogen Field

Depicted at left is a tissue sheet in which a stripe of cells (orange) produces a morphogen that spreads over a distance of approximately 40 cell bodies (blue). This situation approximates the Dpp gradient observed in the wing discs of third instar *Drosophila* larvae. In the middle panel, this arrangement is replaced by a homogenous distribution of receptors (R) in a two-dimensional space adjacent to a linear morphogen source. At right, this situation is further simplified to a one-dimensional model with constant morphogen production at $x = 0$, absorption at $x = x_{max}$, and an initially uniform receptor concentration throughout.

in which morphogen is introduced at rate ν at one location, and absorbed at another (Figure 1). To the expression for diffusive transport provided by Fick's second law, $(\partial[L]/\partial t = D\partial^2[L]/\partial x^2$, where [L] is the concentration of the diffusing species, t is time, x is distance, and D a diffusion coefficient), we add terms that incorporate rate constants of receptor binding and dissociation (k_{on} and k_{off}, respectively). Equations 1 and 2 (Figure 2A) are then obtained by letting R_{tot} be the receptor concentration per unit of extracellular space, and letting A and B be the concentrations of free and receptor-bound morphogen, respectively, normalized to R_{tot}. B is thus "fractional receptor occupancy"; the parameter that, ultimately, needs to be graded.

After specifying initial and boundary conditions, equations 1 and 2 may be solved for various times following onset of morphogen synthesis. In Figure 3, the morphogen field is 100 μm (about the size of the Dpp field in the fly wing disc), and the effective diffusion coefficient (D') is 10^{-7} cm^2 s^{-1} (4- to 5-fold lower than predicted for a molecule the size and shape of Dpp or its vertebrate ortholog BMP-2 [Groppe et al., 1998; Scheufler et al., 1999], reflecting adjustment for tissue tortuosity [see Experimental Procedures]).

In Figure 3A, in which parameter values approximate those of Kerszberg and Wolpert (1998), free morphogen rapidly forms a broad gradient from source to sink, but bound morphogen appears in a steep wave that sweeps from left to right. As this wave passes over any location, receptors go from being largely unoccupied ($B \approx 0$) to nearly saturated ($B \approx 1$). A broad gradient of receptor occupancy never occurs, precisely as Kerszberg and Wolpert (1998) assserted. By varying parameters, one can make the waves of receptor occupancy flatter (Figures 3B and 3D), or slower moving (Figures 3C and 3D), but eventually receptors become filled nearly everywhere.

As it happens, this behavior is well known for systems that combine diffusion and adsorption (Cussler, 1997) but is less a consequence of the presence of absorbers (receptors) than of inadequate means to remove the adsorbing species (the morphogen). In living tissues, molecules that bind receptors do not simply stay bound—they are endocytosed and degraded. Indeed, in the wing disc, extracellular Dpp turns over rapidly (Teleman and Cohen, 2000), and endocytosis is required to form a proper gradient (Entchev et al., 2000).

To allow for constitutive (not ligand-induced) internalization and degradation of morphogen-receptor complexes, we replace equation 2 with 2′ (Figure 2B), introducing rate constant k_{deg}. Since extracellular Dpp in the *Drosophila* wing disc is degraded almost completely within 3 hr (Teleman and Cohen, 2000), we infer that $k_{deg} \geq 10^{-4}$ s^{-1} in that system.

In Figure 4, the scenarios in Figure 3 have been recalculated with $k_{deg} = 2 \times 10^{-4}$ s^{-1}. The results are virtually unchanged when the rate of morphogen production is high (compare Figures 4A and 4B with 3A and 3B), but when it is low (Figures 4C and 4D), we now obtain steady-state gradients of receptor occupancy. In one case (Figure 4D), the gradient profile is much like that of Dpp-GFP in the fly wing disc (Entchev et al., 2000; Teleman and Cohen, 2000).

Analysis shows that steady-state gradients form whenever the rate of introduction of morphogen into the system (ν) is slower than receptor turnover ($k_{deg}R_{tot}$). One can calculate the shapes of such gradients by setting the time rates in equations 1 and 2′ to zero. Rearranging, we see that B depends on only two parameters:

$$\beta = \frac{\nu}{R_{tot}k_{deg}}; \text{ and } \psi = \frac{x_{max}^2\, k_{deg}}{D'} \frac{k_{on}R_{tot}}{(k_{off} + k_{deg})}.$$

For all steady-state gradients, $\beta < 1$; β also happens to equal fractional receptor occupancy at the start of the gradient (i.e., B at $x = 0$). Figures 5A and 5B show steady-state gradients of receptor occupancy for several values of β and ψ. For every β, larger ψ makes gradients steeper at the outset, and smaller ψ makes them shallower.

Since not all gradient shapes will be biologically useful (i.e., able to broadly distribute patterning information over the entire field of cells), we develop a criterion, η (see Experimental Procedures for definition), such that $\eta < 0.5$ categorizes those profiles that are either initially "too steep" or "too shallow" (i.e., the gradient falls over too narrow a range to be biologically useful). Figure 5C

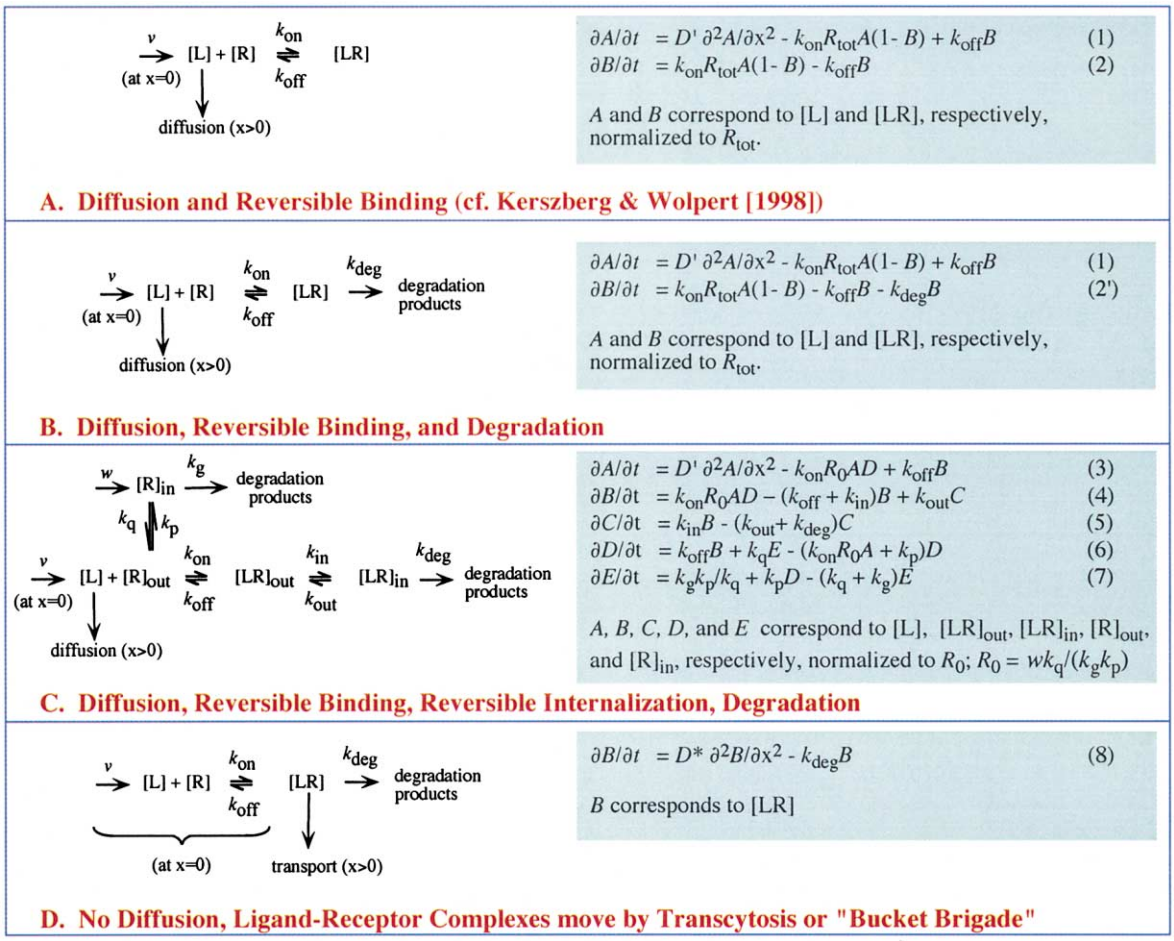

Figure 2. Potential Mechanisms of Morphogen Transport

(A) Diffusive transport of ligand L that reversibly binds receptor R to form complex LR. Ligand enters the system at a constant rate ν at $x = 0$, and absorbed at $x = x_{max}$. D′ is the diffusion coefficient adjusted for tissue tortuosity (see Experimental Procedures). Receptor concentration is constant at all x. This system replicates the key features of that studied by Kerszberg and Wolpert (1998).

(B) Diffusive transport of ligand L that reversibly binds receptor R to form complex LR, where LR is degraded with first order kinetics. Other conditions are as in (A).

(C) Diffusive transport of ligand L that reversibly binds receptor R_{out} to form complex LR_{out}, which can be reversibly internalized to become LR_{in}. LR_{in} is degraded with first order kinetics. Ligand is produced at a constant rate at $x = 0$, and absorbed at $x = x_{max}$. We can no longer take the concentration of receptors to be a constant, and instead describe it in terms of a balance between synthesis (w) and degradation (k_g). R_{out} is determined by R_{in} in accordance with receptor-specific rates of exocytosis and internalization. By introducing R_0 (R_{out} at $t = 0$) into the equations it is possible to eliminate w.

(D) Proposed transport of ligand-receptor complexes by transcytosis or bucket brigade mechanisms, in the absence of diffusibility of free ligand. Ligand L enters the system at a constant rate ν at location $x = 0$ and can combine with receptors to form LR. The rate of production of LR at $x = 0$ will be ν in the steady state and can never exceed ν. Assuming total receptor levels remain constant, the passage of LR through or around the perimeter of cells, followed by the transfer of ligand from one receptor to another, is equivalent to a process where LR itself is transported from one end of the gradient to another, in accordance with a transport coefficient (D^*) that takes into account both the time for transport over a cell and the time for ligand transfer from cell to cell. We also specify that LR is subject to degradation throughout the morphogen field. As in (A)–(C), we add a boundary condition that LR is absorbed at $x = x_{max}$.

illustrates those combinations of β and ψ that produce "useful" ($\eta \geq 0.5$) steady-state receptor occupancy gradients. We may then ask which combinations are physiologically plausible.

With respect to β, we note that values close to 1 are problematic, since small fluctuations in morphogen synthesis (ν) or receptor concentration (R_{tot}) could cause stable gradients to become unstable. Physiological levels of β are likely to be <0.8 (80% receptor occupancy at the top of the gradient), but may in fact be much lower (Dyson and Gurdon, 1998).

As for ψ, we note that morphogens that bind tightly will get internalized and degraded before they dissociate (i.e., $k_{off} < k_{deg}$), so that $\psi \approx x_{max}^2 k_{on} R_{tot}/D'$. Assuming $D' = 10^{-7}$ cm^2 s^{-1} and $x_{max} = 0.01$ cm, then $\psi \approx 1000\, k_{on}R_{tot}$. With $R_{tot} \approx 3.3 \times 10^{-10}\, \rho$, where ρ is the number of receptors per cell (see Experimental Procedures), then $\psi \approx 3.3 \times 10^{-7} k_{on}\, \rho$. Using this relationship, we plot, in Figure 5D, combinations of β and k_{on} that, for any given ρ, produce useful ($\eta \geq 0.5$) gradients. The interesting result is that such gradients require values of k_{on} and numbers of receptors per cell that are at the low end of

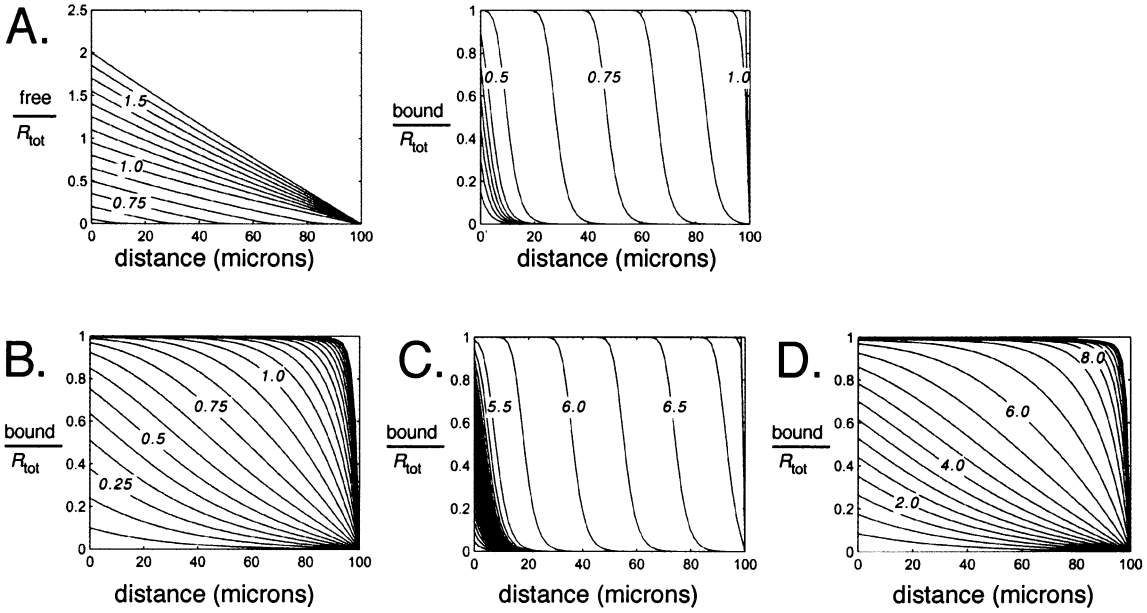

Figure 3. Gradients Produced by the Mechanism in Figure 2A

Equations 1 and 2 were solved with initial conditions $B = 0$ for all x, and $A = 0$ for all $x \neq 0$; and boundary conditions $A = B = 0$ at $x = x_{max}$ and $\partial A/\partial t = \nu/R_{tot} - k_{on}R_{tot}A(1 - B) + k_{off}B$ at $x = 0$. In all cases, D' was taken to be 10^{-7} cm^2 s^{-1} and $x_{max} = 0.01$ cm (100 μm).

(A) Values of A (free morphogen/R_{tot}) and B (bound morphogen/R_{tot}, i.e., fractional receptor occupancy) as a function of distance and time for the following parameters (in units of s^{-1}): $\nu/R_{tot} = 5 \times 10^{-4}$, $k_{on}R_{tot} = 1.32$, and $k_{off} = 10^{-6}$.

(B–D) Values of B (fractional receptor occupancy) as a function of distance and time for the following sets of parameters (all in units of s^{-1}). (B) $\nu/R_{tot} = 5 \times 10^{-4}$, $k_{on}R_{tot} = 0.01$, $k_{off} = 10^{-6}$; (C) $\nu/R_{tot} = 5 \times 10^{-5}$, $k_{on}R_{tot} = 1.32$, $k_{off} = 10^{-6}$; (D) $\nu/R_{tot} = 5 \times 10^{-5}$, $k_{on}R_{tot} = 0.01$; $k_{off} = 10^{-6}$. In (A) and (B), the time interval between successive curves is 300 s; in (C) it is 900 s; in (D) it is 1800 s. The cumulative time represented by selected curves is shown in hours by legends directly atop those curves.

what one typically sees with ligands that bind cell surface receptors. For example, if epidermal growth factor ($k_{on} = 3 \times 10^6$ M^{-1} s^{-1} [Lauffenburger and Linderman, 1993]), had to make a useful gradient over 100 μm that occupied $\leq$70% of cell surface receptors at its highest point ($\beta \leq 0.7$), the lower bound on ψ would constrain the number of receptors per cell (ρ) to be $<$54. Of these, at most 38 ($\rho \times \beta$) would be occupied at the start of the gradient, and even fewer else where (for example, if $\eta = 0.5$, then halfway into the morphogen field at most five receptors per cell would be occupied).

It is doubtful that such low receptor occupancy could

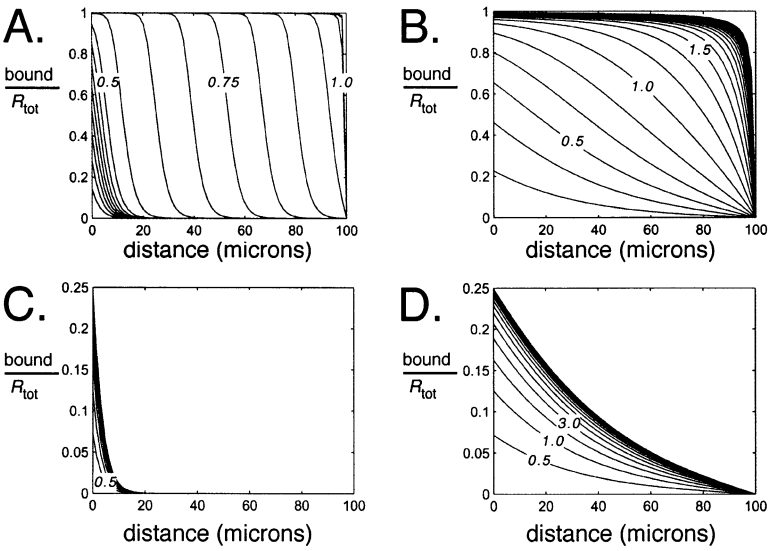

Figure 4. Gradients Produced by the Mechanism in Figure 2B

Equations 1 and 2′ were solved with the same initial and boundary conditions and values of D' and x_{max} as in Figure 2. The additional parameter k_{deg} was set to 2×10^{-4} s^{-1}. Values of B (fractional receptor occupancy) are plotted as a function of distance and time for the following parameters (in units of s^{-1}): (A) $\nu/R_{tot} = 5 \times 10^{-4}$, $k_{on}R_{tot} = 1.32$, $k_{off} = 10^{-6}$; (B) $\nu/R_{tot} = 5 \times 10^{-4}$, $k_{on}R_{tot} = 0.01$, $k_{off} = 10^{-6}$; (C) $\nu/R_{tot} = 5 \times 10^{-5}$, $k_{on}R_{tot} = 1.32$, $k_{off} = 10^{-6}$; and (D) $\nu/R_{tot} = 5 \times 10^{-5}$, $k_{on}R_{tot} = 0.01$; $k_{off} = 10^{-6}$. In (A), the time between successive curves is 300 s; in (B) it is 600 s; in (C) and (D) it is 1800 s. The cumulative time represented by selected curves is shown in hours by legends directly atop of those curves. The curves in (C) and (D), unlike those in (A) and (B), approach a steady-state receptor occupancy gradient. In both (C) and (D), receptor occupancy at $x = 0$ achieves 80% of its steady-state value in $\sim$2.25 hr. In (D), receptor occupancy at $x = 50$ μ achieves 80% of its steady-state value in $\sim$3.25 hr.

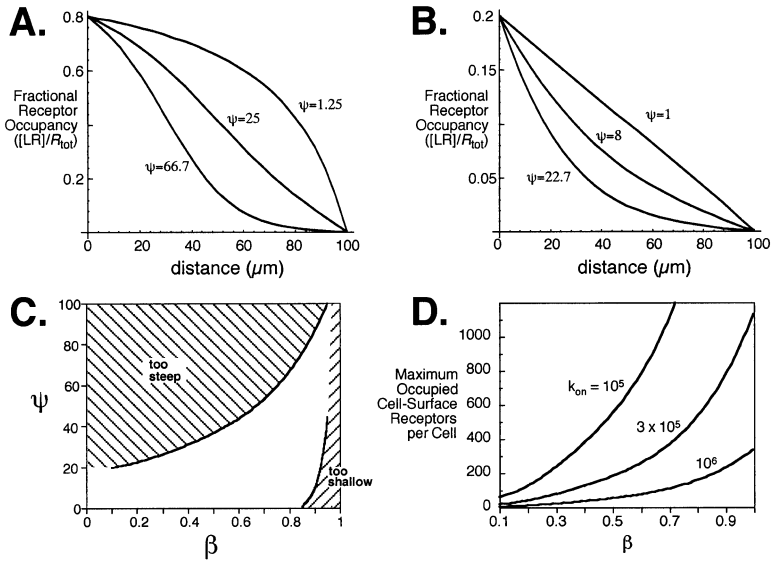

Figure 5. Parameters that Affect the Shapes of Steady-State Receptor Occupancy Gradients

(A and B) Steady-state gradients predicted by the equations of Figure 2B. Each curve shows a particular combination of the parameters ψ (values next to each curve) and β (0.8 in [A] and 0.2 in [B]). The lowest curves in each panel (marked $\psi = 66.7$ in [A] and $\psi = 22.7$ in [B]) demarcate the proposed cut off ($\eta \geq 0.5$) for gradients broad enough to be biologically useful.

(C) Values of ψ associated with curves that meet the criterion $\eta = 0.5$ are plotted as a function of β for all values of β that permit formation of steady-state gradients. Ranges of ψ and β that give gradients of receptor occupancy that initially decline too quickly ("too steep") or slowly ("too shallow") are marked.

(D) Cut-off values of ψ for gradients that are "too steep" in (C) were converted to values of ρ (receptors per cell) for three different values of k_{on} (units of $M^{-1}\ s^{-1}$) and multiplied by β to yield numbers of occupied cell surface receptors per cell at the highest points of the predicted gradients (i.e., $x = 0$). Minimum levels of receptor occupancy needed to detect a morphogen are thought to be on the order of 100/cell (Dyson and Gurdon, 1998). Presumably, occupancy at the high point of a gradient would need to be substantially higher than this (to ensure minimum occupancy at distant locations). These data suggest that only relatively slow association rate constants ($k_{on} \leq 3 \times 10^5\ M^{-1}\ s^{-1}$) are compatible with achieving both sufficiently broad gradients and adequate levels of cell surface receptor occupancy.

mediate morphogen signaling. An embryonic *Xenopus* cell requires occupation of ≥100 receptors just to detect activin (Dyson and Gurdon, 1998; Gurdon et al., 1998). Thus, to generate useful gradients by diffusion, it would seem that organisms would be best served by using morphogens with slow association kinetics. Intriguingly, known morphogens—such as activins, BMPs 2 and 4 (the vertebrate orthologs of Dpp), and related members of the TGF-β superfamily—all exhibit slow association and dissociation kinetics, among the slowest known for polypeptide growth factors (De Crescenzo et al., 2001; Dyson and Gurdon, 1998; Iwasaki et al., 1995). Using $k_{on} \approx 10^5\ M^{-1}\ s^{-1}$ for BMPs 2 and 4 (Iwasaki et al., 1995; Lander, 1999; Natsume et al., 1997) in the above analysis, we come up with a more acceptable maximum of 1620 receptors/cell (for $\beta = 0.7$, $\eta = 0.5$), with 1134 occupied at the start of the gradient and 158 occupied half way in.

It would thus seem that nature has enlisted as morphogens just the kinds of molecules that allow gradients to form by diffusion. It would also seem that, even with slowly associating morphogens, levels of receptor expression still need to be rather low (e.g., <1000–2000/cell). This is another prediction that agrees well with observation: in developing *Drosophila*, expression of the Dpp receptor Thickveins (as assessed by in situ hybridization) is quite high at many times and locations, but almost undetectable in precisely those locations where cells are patterned by Dpp gradients (Brummel et al., 1994; Lecuit and Cohen, 1998).

As the data in Figure 5 concern only steady-state gradients, we need also consider whether the rate of formation of such gradients fits the in vivo data. As shown in Figure 4D, for a typical case with reasonable values of steady-state receptor occupancy, cells half way into the morphogen field achieve 80% of those values by 3.25 hr. This is within the range of measurements made for Dpp-GFP in the wing disc (Entchev et al., 2000; Teleman and Cohen, 2000).

Significance of Intracellular Morphogen Accumulation

The above calculations assume that internalized morphogen-receptor complexes are instantly degraded. Yet many internalized ligand-receptor complexes continue to signal, from within endocytic compartments, for long times, followed either by return to the cell surface or destruction (Leof, 2000). Figure 2C modifies the previous model (Figure 2B) to permit such events. It also discards the assumption that rates of receptor internalization are constant (for the Dpp ortholog BMP2 it is known that ligand binding increases receptor internalization [Jortikka et al., 1997]). As these changes allow the receptor concentration to vary over time, we can no longer represent it with a constant (R_{tot}). Instead, we explicitly account for appearance and disappearance of cell surface receptors by synthesis, exocytosis, endocytosis, and degradation. In all, five equations determine the system, with subscripts "out" and "in" specifying cell surface and intracellular locations, respectively, of receptors and ligand-receptor complexes. For convenience, we introduce R_0, the initial cell surface receptor concentration prior to the onset of morphogen synthesis (i.e., $[R]_{out}$ at $t = 0$). *A, B, C, D,* and *E* are then used to represent [L], $[LR]_{out}$, $[LR]_{in}$, $[R]_{out}$, and $[R]_{in}$, respectively, normalized to R_0. Thus, both *B* and *C* quantify signaling complexes.

It should be noted that here k_{deg}, the rate constant for degradation of internalized ligand-receptor complexes ($[LR]_{in}$), is not something investigators commonly observe. For example, Teleman and Cohen (2000) labeled

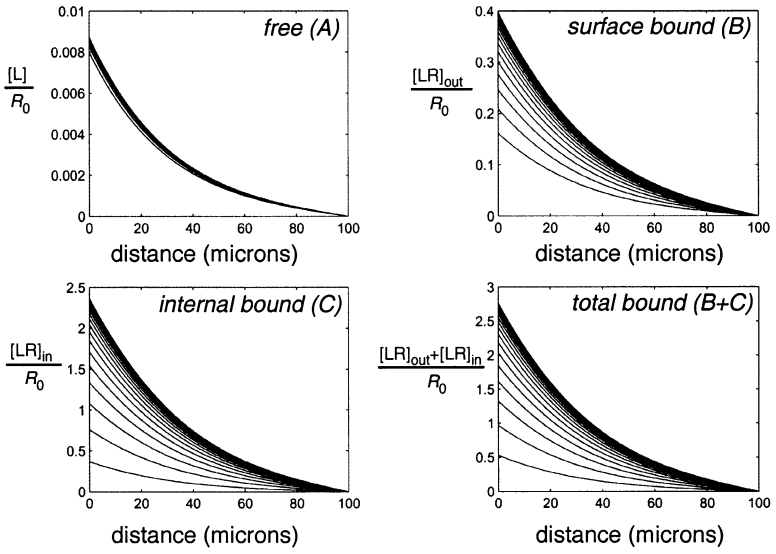

Figure 6. One Solution to the Equations of Figure 2C

Shown are gradients of *A* (free morphogen/R_0), *B* (morphogen bound to cell surface receptors/R_0), *C* (morphogen bound to internalized receptors/R_0), and *B* + *C* (total bound morphogen/R_0). Curves are separated by intervals of 2 hr. Parameters were $D' = 10^{-7}$ cm^2 s^{-1}, $x_{max} = 100$ μm, and, in units of sec^{-1}: $\nu/R_0 = 8 \times 10^{-5}$, $k_{on}R_0 = 0.012$, $k_{off} = 10^{-5}$, $k_{deg} = 3.3 \times 10^{-5}$, $k_p = 6 \times 10^{-4}$, $k_q = 5 \times 10^{-5}$, $k_{in} = 6 \times 10^{-4}$, $k_{out} = 6.7 \times 10^{-5}$, and $k_g = 10^{-4}$. These parameters imply $k_{deg,obs} = 2 \times 10^{-4}$ s^{-1}, $\beta = 0.2$, $\psi = 11.36$, and $\eta = 0.69$. Initial conditions were $A = B = C = 0$, $D = 1$, and $E = k_p/k_q$. The last two initial conditions follow from the definition of R_0 and equations 6 and 7. As before, we add the boundary condition that all morphogen is absorbed at $x = x_{max}$. Note the different ordinate scales for *A*, *B*, and *C*, which imply that, at steady state, over 99% of morphogen is bound and 86% of that is present inside cells. Interestingly, if k_{on} is to be at least 1.2×10^5 M^{-1}s^{-1}, then the initial number of cell surface receptors per cell (R_0) in this case must be $\leq$303 (see Experimental Procedures). Since the values for *A*, *B*, and *C* are normalized to R_0, we can infer maximum possible steady-state values of total receptor occupancy per cell as $303(B + C) = 848$, at $x = 0$. At $x = 2/3\ x_{max}$, it would be 105. In contrast, in the previous model (Figure 2B), parameters of $\beta = 0.2$, $\psi = 11.36$, and $\rho = 303$ would have yielded maximum receptor occupancies of 61 per cell at $x = 0$ and 8 per cell at $x = 2/3\ x_{max}$, values that are probably too low to be biologically plausible. These calculations illustrate how allowing substantial fractions of morphogen-receptor complexes to build up inside cells permits cells to display fewer receptors on the cell surface, which in turn relieves some of the constraints placed on k_{on} (Figure 5). It should be noted that none of the trafficking rate constants used in this example exceed values documented in cultured cells for EGF-EGF receptor trafficking (Lauffenburger and Linderman, 1993).

Dpp by cell surface biotinylation and followed its fate; in effect, they quantified the loss of $[LR]_{out}$. One can show that, in the system described above, the steady-state degradation rate constant for $[LR]_{out}$ is $(k_{in}k_{deg}/(k_{out} + k_{deg}))$, a quantity we will therefore call $k_{deg,obs}$.

Although the equations in Figure 2C are more numerous than those in Figure 2B, in the steady state they produce the same curves, albeit with modified definitions of β and ψ and a change in scale. Specifically, if one wishes to plot total receptor occupancy (i.e., $B + C$), then the shapes of gradients are the same as those for Figure 2B, except that now:

$$\beta = \frac{\nu}{R_0 k_g}\frac{(k_q + k_g)}{k_p}; \text{ and } \psi = \frac{x_{max}^2 k_{deg,obs}}{D'}\frac{k_{on}R_0}{(k_{off} + k_{deg,obs})}.$$

Again the steady-state condition is $\beta \leq 1$, but the curves are scaled so that β no longer corresponds to receptor occupancy at the start of the gradient ($x = 0$).

Clearly, allowing ligand-induced receptor endocytosis and persistent signaling by internalized receptors neither prevents formation of stable receptor occupancy gradients nor alters the possible steady-state profiles. It does, however, allow for gradients in which much of the morphogen is found inside cells (complexed with receptors), an example of which is illustrated in Figure 6. Such localization, of course, is exactly what has been observed with Dpp-GFP in *Drosophila* wing discs (Entchev et al., 2000; Teleman and Cohen, 2000).

Interestingly, these modifications not only explain how diffusion-generated morphogen gradients can be populated mainly by intracellular morphogens, they also help overcome a limitation of the previous system (Figure 2B). In that case, to avoid making gradients too steep (ψ too large), it was desirable to have low numbers of receptors per cell. Yet limits on how low receptor numbers could go before losing response to the morphogen made it necessary to also employ morphogens with very slow rates of receptor binding (Figure 5D).

In the modified system, since many ligand-receptor complexes can exist inside the cell, the number of occupied receptors is no longer limited to those at the surface. Thus, cells have the option to keep very few free receptors at the surface (thus hindering morphogen diffusion less), yet still achieve high levels of signaling. This behavior is also exhibited in Figure 6 (see legend).

In short, in systems where morphogen gradients form by diffusion, buildup of morphogens inside cells is not only permissible, it is biologically advantageous, as it allows greater flexibility in receptor kinetics (i.e., k_{on}) and signal sensitivity. Intracellular morphogen buildup cannot then be taken as evidence against diffusive transport.

Do Results from Blocking Receptor Internalization Favor Transcytotic Transport?

The strongest arguments against diffusive morphogen transport come from experiments in which blocking endocytosis causes defects in morphogen gradient formation (or subsequent tissue patterning). In *Drosophila*, temperature-sensitive mutations in the *shibire* (dynamin) gene provide a convenient tool for this (Chen et al., 1991; van der Bliek and Meyerowitz, 1991).

Using this approach in the wing disc, González-Gaitan and Jäckle (1999) and Entchev et al. (2000) showed that endocytic blockade disrupts the Dpp gradient (and its patterning effects) and results in an overall decrease in

Dpp in the morphogen field. Obviously, this result is consistent with a transcytotic (endocytosis-driven) mechanism of Dpp transport. Yet a diffusive transport model makes similar predictions: without internalization, no degradation can occur and therefore no steady state can be reached (Figure 3), nor can cells build up high levels of intracellular morphogen-receptor complexes (as in Figure 6).

Potentially more telling experiments are those testing the ability of Dpp-GFP to propagate through clones of *shibire* mutant cells (Entchev et al., 2000). During gradient formation, such clones not only failed to accumulate normal levels of Dpp-GFP within them, they also produced "shadows" of low fluorescence behind them (with respect to the Dpp source). Eventually, the shadows filled in; this was ascribed to the fact (established by other experiments) that transport is nondirectional and therefore can fill in Dpp from beside or beyond the shadows.

At first glance, such shadows seem to argue compellingly against diffusive transport. Why should freely diffusing Dpp be retarded by a clone of cells incapable of internalizing it? If anything, one might guess it would diffuse more readily past such a cells, yet on closer inspection, the equations of Figure 2C tell another story. Since the concentration of receptors at the cell surface is determined by a balance of synthesis and degradation, a blockade of endocytosis should increase the number of receptors at the cell surface. This, in turn, should affect Dpp diffusion.

In fact, loss of *shibire* function is known to cause increased cell surface receptor levels: in embryos carrying *shibire*^{ts} mutations, cell surface levels of the Hedgehog receptor Patched increase dramatically after only 40 min at a restrictive temperature (Capdevila et al., 1994). Likewise, in *Drosophila* oocytes, exogenously expressed transferrin receptors shift from being mainly intracellular to mainly plasmalemmal in response to loss of *shibire* function (Bretscher, 1996). These findings are consistent with evidence that only endocytosis, not exocytosis, is blocked in *shibire* mutants (Koenig and Ikeda, 1996).

How significantly should Dpp diffusion through a *shibire* mutant clone be affected by an increased numbers of cell surface receptors? Since gradient shape depends largely on ψ, which varies in proportion to cell surface receptor concentration, one would expect gradients to fall more steeply through such clones. If they fell steeply enough, one should see "shadows" behind the clones. We can show this by solving equations 3–7 with the condition that, between $x = 0.25x_{max}$ and $0.5x_{max}$ (i.e., a "clone" of $\sim$10 cells across), all internalization rate constants (k_p, k_{in}) are substantially and equally reduced. Over the same interval, we alter our initial conditions to reflect the fact that cell surface receptor levels will be elevated, potentially by as much as the same factor by which k_p and k_{in} were lowered.

The results are shown in Figure 7, which otherwise uses the parameters of Figure 6. Concentration profiles are plotted for intracellular and cell surface occupied receptors (*C* and *B*, respectively, in equations 3–7). Superimposed upon the "experimental" curves (in which endocytosis was inhibited in the "clone") are control curves (dashed lines) in which no parameter changes were made. One can think of the experimental and control curves as cross-sections through a wing disc at levels through the middle of a *shibire* clone, and far from such a clone, respectively.

The first two panels in Figure 7 show results 5 hr after the onset of morphogen synthesis. One can clearly see that internal and surface-bound morphogen levels are lower "behind" the "clone" in the experimental curves. In other words, a model in which transport occurs only by diffusion predicts the same type of shadow that Entchev et al. (2000) saw, at the same time (5 hr) at which they saw it. Because the observations of Entchev et al. (2000) were made using procedures that emphasized intracellular morphogen (e.g., by using optical sections at the apical extremes of cells, where intravesicular Dpp-GFP is highly concentrated, and by emphasizing punctate accumulations [Entchev et al., 2000]), their observations are best modeled by the curves labeled "internal bound". Since they were only able to detect cell surface Dpp-GFP under special staining conditions, we suspect that the predicted large increase, within the clone, of surface-bound Dpp (center panel, solid curve) would not have been noticed by them.

The third panel of Figure 7 shows the results for internal morphogen at a later time (24 hr). Note that the shadow behind the "clone" fills in, again in close agreement with observations (Entchev et al., 2000). Although the examples in Figure 7 are selected cases, it is easy to demonstrate these phenomena for a wide variety of parameters consistent with the formation of useful gradients.

These results from modeling *shibire* clones also help explain why one effect of endocytic blockade throughout the *Drosophila* wing disc (whether produced with *shibire* mutations or through other means, such as dominant-negative rab proteins) is a reduction in the range of Dpp signaling (Entchev et al., 2000). Any global increase in cell surface receptor expression would generally be expected to have this effect.

How Plausible Are Nondiffusive Transport Mechanisms?

Apparently, diffusive models of morphogen transport can account for much of the experimental data. Now we ask whether other transport models, such as transcytosis (Entchev et al., 2000; Pfeiffer and Vincent, 1999) and bucket brigades (Kerszberg and Wolpert, 1998), can do likewise.

We begin with a critical observation by Entchev et al. (2000). They made clones of Dpp-GFP-producing cells in the wing disc, and saw Dpp move out in all directions from them. They inferred that however Dpp moves, it must be directionally random (Entchev et al., 2000). Any "random walk" transport process obeys Fick's laws, a consequence of which is that transport times vary with the square of distance (Berg, 1993). Since the Dpp gradient in the wing disc is $\sim$40 cells long, the average time for Dpp to move halfway (20 cells) across that field will be $20^2 = 400$ times that needed to traverse a single cell. Since the Dpp gradient is almost fully established within 7 hr of the onset of Dpp expression (Entchev et al., 2000; Teleman and Cohen, 2000), we may roughly estimate the time to cross a single cell as less than 7 hr $\div$ 400 = 63 s.

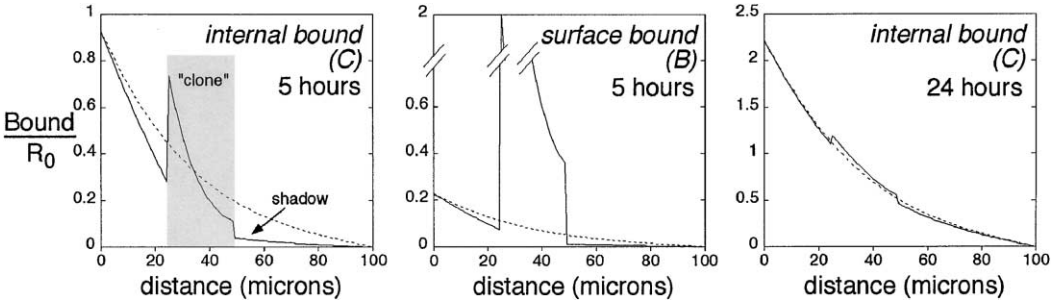

Figure 7. A Clone of Endocytically Impaired Cells Will Hinder Even Diffusive Transport

The model in Figure 2C was solved using the parameters of Figure 6 except that, for the solid curves, a 90% reduction in endocytosis was simulated over the interval from 25 to 50 μm. This was accomplished by decreasing the endocytic rate constants (k_p and k_{in}) by 10-fold and increasing the initial value of D (cell surface receptors) by 10-fold within that interval. The latter change follows from the fact that, at $t = 0$, $[R]_{out} = wk_q/(k_g k_p)$. For comparison, the dashed curves show solutions in which all parameters were left unchanged. The solid curves may be understood as cross-sections through the middle of a 10 cell diameter *shibire* clone, and the dashed curves as cross-sections distant from such a clone. Data are shown for internalized and cell surface morphogen-receptor complexes (as in Figure 6, the concentration of free morphogen is too low to contribute significantly to the total). The results indicate that morphogen diffusion through an endocytically impaired clone is inhibited, transiently producing a "shadow" in the gradient profile from 50 to 100 μm. The shadow is particularly evident at 5 hr, the time when such behavior was observed in vivo (Entchev et al., 2000).

We can be more precise by writing a transport equation (Figure 2D; equation 8) in which B is the concentration of Dpp-receptor complexes and D^* is a "transport coefficient" specific to the transport process (e.g., transcytosis or bucket brigade). The term $k_{deg}B$ is included because cell surface Dpp is rapidly degraded in the wing disc (as discussed earlier, $k_{deg} \geq 10^{-4}$ s^{-1} [Teleman and Cohen, 2000]). Equation 8 can be solved analytically in the steady state, and transiently approximated (see Experimental Procedures).

From transient solutions we learn that, to form gradients that achieve 60% of their steady-state level at $x = 0.5x_{max}$ within 7 hr, we require $D^* > 2.11 \times 10^{-10}$ cm^2 s^{-1}. For cells of 2.5 μ diameter, this implies that Dpp is transported across a single cell in, on average, 148 s or less. From the steady-state solution to equation 8, we learn that, for $k_{deg} \geq 10^{-4}$ s^{-1}, gradients that form are too steep to be biologically useful ($\eta < 0.5$; see Experimental Procedures) unless $D^* > 0.058x_{max}^2 k_{deg}$. For $x_{max} = 0.01$ cm, this implies $D^* > 5.8 \times 10^{-10}$ cm^2 sec^{-1}, or a mean time for Dpp to cross a single cell of <54 s.

Could transcytosis move Dpp from one cell to another in 54, or even 148 sec? Within this time receptor association, internalization, transport through the cell, externalization, and dissociation all must occur. In cultured cells, transcytotic rate constants for transferrin, EGF, and ligands of the polymeric immunoglobulin receptor (Sheff et al., 1999; Shitara et al., 1998) imply mean transit times of 0.6–4 hr. In other cells, internalizing these ligands itself takes 2–20 min (Lauffenburger and Linderman, 1993; Sainte-Marie et al., 1991; Sheff et al., 1999). For known morphogens, activin and BMP4, just dissociating from receptors takes on the order of hours (Dyson and Gurdon, 1998; Lander, 1999; A. Kumbasar and A.D.L., unpublished data).

Could a bucket brigade mechanism move Dpp from one cell to another in 54, or even 148 sec? In this case, receptor diffusion within the plasma membrane is the major means of transport. Given typical planar diffusion coefficients for transmembrane proteins ($D \approx 10^{-10}$ cm^2 s^{-1}), and noting that the shortest path along the plasma membrane from one location on a cylindrical cell to a diametrically opposite one is $\pi/2$ times the diameter, we obtain a mean time to cross a 2.5 μ diameter cell of 771 s. To this, one would still need to add time to transfer Dpp from one receptor to another on an adjacent cell. To occur in under a minute, that process would require kinetics orders of magnitude faster than the unassisted dissociation of BMPs and activins from their receptors (Dyson and Gurdon, 1998; Lander, 1999).

In short, for processes other than diffusion to set up the Dpp gradient in the *Drosophila* wing disc, a series of cell biological events would have to occur at implausibly fast rates.

Discussion

How morphogen gradients arise has attracted much controversy. One argument against a diffusive mechanism has been that unoccupied cell surface receptors strongly retard diffusion (Kerszberg and Wolpert, 1998). As the present study shows, this insight is valid, but when receptor-mediated ligand degradation is taken into account, there are ranges of parameters (i.e., rate constants, receptor numbers, etc.) that do enable stable, biologically useful gradients to form.

A second argument against diffusive transport stems from observations of substantial amounts of morphogen in intracellular compartments (Entchev et al., 2000; Gonzalez et al., 1991; Tabata and Kornberg, 1994; Teleman and Cohen, 2000). Here we show that diffusive transport is not only compatible with such observations, but that internalization of morphogen-receptor complexes actually aids gradient formation by allowing cells to reduce the number of free cell surface receptors without suffering a loss of ability to respond to the morphogen.

A third argument against diffusive morphogen transport stems from observations that interference with endocytosis causes long-range defects in morphogen transport. Here we show that, because endocytic blockade alters cell surface receptor expression, such results

are predicted by models of morphogen transport by diffusion alone.

Finally, we show that transcytosis and bucket brigade transport mechanisms—if they are to be directionally random, as is Dpp-GFP in the *Drosophila* wing disc—have a difficult time explaining existing data, unless one makes mechanistic assumptions that are shaky, at best.

On the basis of these findings, we propose that morphogen gradients can, and in many cases do, form by "simple" diffusion. Other data that support this analysis include observations that overexpressing the Dpp receptor subunit thickveins (Tkv) in clones of cells in the *Drosophila* wing disc inhibits the spread of the Dpp activity gradient (Lecuit and Cohen (1998). This result is directly predicted by the models described here, but not by models in which receptors carry morphogen from cell to cell.

Critique of Assumptions

In deriving equations for this study, some simplifications were made. For example, the tortuous paths taken by diffusing molecules were replaced by a homogeneous receptor-filled space in which the diffusion coefficient D' is 4- to 5-fold lower than predicted for free solution. This is justified by theoretical studies and empirical observations in other tissues (see Experimental Procedures). If intercellular pathways are less tortuous (e.g., possessing oriented channels) or extracellular fluid less viscous, we may be slightly underestimating D'. However, the small effect on ψ would not alter the general conclusions of this study.

Alternatively, we may be overestimating D'. Many morphogens are "sticky" proteins, interacting with various nonreceptor sites in tissues (e.g., proteoglycans [Baeg and Perrimon, 2000]). A full analysis of how such sites affect gradient formation will be given elsewhere, but preliminary analyses show that such nonreceptor interactions cannot simply be equated with a decrease in D'. Indeed, depending on kinetic parameters, the effects of such interactions on steady-state gradients of receptor occupancy can be relatively minor, even when nonreceptor sites are very abundant (our unpublished data).

In the present study, a relationship was derived between receptor concentrations in extracellular space (R_{tot}, R_0) and cell surface receptor density (ρ) that relied upon assumptions about the extracellular volume fraction (see Experimental Procedures). It is straightforward to calculate the effects of differences in this parameter. For example, for a given cell surface receptor density, a 50% decrease in the space between cells would result in a 2-fold increase in ψ, which would yield steeper gradients.

Extension to Other Morphogen Systems

Although many of the results above refer to the Dpp gradient in the *Drosophila* wing disc, we can discern hallmarks of diffusive transport in other morphogen systems. For example, *Drosophila* wingless (Wg), a homolog of vertebrate Wnts, is distributed in a graded fashion in both embryo and imaginal discs. In embryos, blockade of endocytosis causes decreased Wg movement and accumulation of extracellular Wg around endocytically impaired cells (Moline et al., 1999). As discussed above, both results are predicted by diffusive transport; indeed, Wg accumulation around endocytically blocked cells strongly suggests increased cell surface levels of receptors or other Wg binding proteins, which would be likely culprits in hindering transport. Other observations consistent with diffusive transport include: (1) overexpression of receptors interferes with the spread of Wg protein in *Drosophila* embryos (Moline et al., 1999); (2) extracellular Wg is degraded rapidly in discs ($t_{1/2} < 3$ hr) and forms gradients over 50 μ within 1 hr (Strigini and Cohen, 2000); and (3) endocytic blockade does not preclude the formation of Wg gradients (Strigini and Cohen, 2000). On the other hand, in some studies, Wg gradients have behaved in unexpected ways, for example expanding in wing discs in response to receptor overexpression (Cadigan et al., 1998); such phenomena may reflect the additional complexity that comes from feedback effects of Wg signaling on the stability of Wg protein.

For Wg, it is also the case that direct arguments against transcytotic or bucket brigade transport cannot be made as compelling as they can for Dpp in wing discs. In the embryo, at least, Wg gradients act over distances of just a few cells (Lawrence, 2001; Moline et al., 1999), short enough that transcytotic machinery might be sufficiently fast. Ultimately, we must consider the possibility that a single morphogen moves by different means in different situations (e.g., embryos versus wing discs). This seems particularly likely for morphogens such as Hedgehogs, which exist in forms of very different solubility (Zeng et al., 2001), act over a range of distances (Chuang and Kornberg, 2000), and depend on nonreceptor molecules for their transport (The et al., 1999).

We also note that, in some organisms, morphogens act over distances much larger than those in fly wing discs (e.g., hundreds of microns in *Xenopus* embryos [Gurdon and Bourillot, 2001]). This creates challenges for diffusive transport, since achieving useful gradients requires keeping ψ, which scales with the square of distance, small (Figure 5C). In wing discs, this meant values of k_{on} and ρ at the low end of what seemed plausible. For similar gradients to form over three times the length in frog embryos, it might seem that $k_{on}\rho$ would need to be 9-fold lower still.

How might developing animals overcome this problem? It turns out the answer is simple: bigger cells. The concentration of receptors in extracellular space (the quantity that directly affects ψ) is not just proportional to cell surface receptor density (ρ), but inversely related to cell volume (see Experimental Procedures). Given that animal cap cells of early gastrula stage *Xenopus* embryos are cuboidal cells of about $30 \times 30 \times 50$ μ (Hausen and Riebesell, 1991) (about 1000 times the volume of cells of the fly wing disc), there should be no difficulty in generating substantially longer gradients even if k_{on} and ρ are quite a bit higher than in wing discs (for activin receptors on animal cap cells it has been estimated that $\rho \approx 5000$ [Dyson and Gurdon, 1998]). This seems to be another example in which biological observations (i.e., that longer gradient fields have bigger cells) fit well with

the constraints imposed by diffusive models of morphogen transport.

Additional Levels of Control in Gradient Formation

Although diffusive transport can explain most observations of morphogen gradients, at least one result does not fit: Entchev et al. (2000) made clones in the wing disc that lacked the Dpp receptor subunit thickveins (Tkv). Dpp-GFP levels increased sharply within the clones at one edge (facing the Dpp source) and fell sharply thereafter. They viewed this as evidence for transcytotic transport, arguing that Dpp carried to the near edge of such clones could be moved no further (due to lack of receptors) and so simply stopped, accumulating because free Dpp (in their model) is relatively nondiffusible.

Intuitively, this explanation seems reasonable, but in reality it is not. Because the Dpp transport machinery is nondirectional (a fact established by the same authors [Entchev et al., 2000]), there should never be concentration increases at boundaries where transport is blocked, because any accumulation at such a boundary would be relieved by transport in the opposite direction (this follows directly from Fick's laws [Cussler, 1997]). Accordingly, the results obtained with *tkv* null clones cannot be explained by any nondirected transport mechanism, whether it be transcytosis or diffusion.

What then is the explanation? Obviously, Dpp accumulating at near edges of *tkv* null clones is binding to something, possibilities for which include type II receptor subunits and proteoglycans (e.g., dally [Jackson et al., 1997]). If expression of either of these is upregulated in *tkv* clones (i.e., in response to the lack of Dpp signaling), that could explain the Dpp accumulation. The increased level of Dpp binding molecules would also be expected to impede diffusion (as discussed earlier for *shibire* clones), potentially explaining the steep drop in Dpp concentration across the clones.

How likely is it that Dpp signaling regulates the expression of Dpp-type II receptors and/or Dpp binding proteins on cells within the wing disc? Data on this point are lacking, but interestingly, Dpp is known to regulate expression of *tkv* itself (Lecuit and Cohen, 1998). An area ripe for further analysis concerns the effects of such "feedback" regulatory phenomena on morphogen transport. An intriguing possibility is that such effects underlie some of the still unexplained properties of morphogen gradients, such as their intrinsic ability to expand or contract in response to manipulations that increase or decrease the size of the field of responsive cells (Teleman and Cohen, 2000). Such "self-scaling" is critical to the coordination of growth and patterning, a fundamental problem in development.

Experimental Procedures

Simplifying Assumptions

In tissues, secreted molecules diffuse along channels between cells (Figure 1, left panel), the "walls" of which contain receptors. If the rate at which morphogens bind receptors is slow compared with diffusion, we may treat receptors as homogeneously distributed in the volume in which morphogen diffuses (Lauffenburger and Linderman, 1993). Since having receptor binding kinetics well below the diffusion limit turns out to be essential for establishing useful morphogen gradients by diffusion (see Results), this assumption can be made in all interesting cases.

The effects of tortuous, diffusive paths can be captured by a number λ, the geometric tortuosity, representing the fold increase in diffusive path lengths as a result of physical obstacles. The apparent diffusion coefficient, D', of a molecule is thus equal to its free diffusion coefficient D divided by λ^2. In various tissues $\lambda \approx 1.5$–1.8, and mathematical treatments (Rusakov and Kullmann, 1998) suggest that geometry can produce values no higher than this. Apparent diffusion coefficients will also be reduced by viscous effects, either due to true viscosity of intercellular fluid or reversible interactions of morphogen with immobilized molecules. For these reasons, we take D' to be 4- to 5-fold lower than expected for free aqueous diffusion of a medium-sized globular protein, but note that values still lower are possible.

With the above assumptions, we treat morphogen diffusion as occurring in an isotropic environment in which receptors are uniformly distributed at a concentration equal to their actual concentration in the extracellular space, R (Figure 1, middle). Biologists more often express cell surface receptor concentration in units of molecules per cell, which we call ρ. R and ρ are related: $R = \rho(1 - \epsilon)/(V N_A \epsilon)$, where V is volume per cell, ϵ the extracellular volume fraction (the fraction of tissue volume not accounted for by cells, i.e., the intercellular space), and N_A is Avogadro's number. From images of late third instar *Drosophila* wing discs (Eaton et al., 1995; Poodry and Schneiderman, 1970), we estimate $V \approx 15$ – 25 fl. Although ϵ has not been widely measured in developing tissues, for many mature tissues $\epsilon \approx 0.2$ (Nicholson and Sykova, 1998; Rusakov and Kullmann, 1998). Electron micrographs (Poodry and Schneiderman, 1970) suggest that, in fly imaginal discs at least, it is unlikely to be substantially higher than this. Accordingly, we estimate R in the range of 2.6–$4.4 \times 10^{-10}\ \rho$. In figures where relevant, $R = 3.3 \times 10^{-10}\ \rho$ has been used.

We further note that, in fields such as the fly wing disc, transport occurs in an essentially two-dimensional space. Because morphogen sources in the wing disc consist of a linear array of cells in the center of the disc, and we are primarily interested in the formation of gradients perpendicular to such lines (e.g., in the case of Dpp, along the antero-posterior axis), we may consider morphogen gradient formation as a one-dimensional problem (Figure 1, right). This is tantamount to assuming the linear source of morphogen has infinite extent. It creates problems near the edges of the morphogen field, but according to preliminary calculations (data not shown), the effects at most locations are small for cases involving physiologically relevant parameters.

Numerical Solutions

Transient solutions to systems of partial differential equations were obtained using standard finite difference methods (Strikwerda, 1989). Spatial derivatives for the unknowns were approximated by a second-order central difference scheme. A fourth-order Adams-Moulton predictor-corrector method was implemented for the temporal marching. Numerical resolution studies show that the numerical method is second-order accurate in space and fourth-order accurate in time.

Steady-state solutions were also calculated by a shooting method (Keller, 1992) in which a fourth-order Runge-Kutta scheme with a bisection method was incorporated. The steady-state solutions computed from the transient study were compared with the direct steady-state calculations to validate both numerical simulations.

Criteria for "Biologically Useful" Gradients

To distribute a set of cell fates over a field of cells, a morphogen gradient must produce receptor occupancy that is substantially different at locations adequately far apart (Dyson and Gurdon, 1998). Linear gradients provide for the greatest spread of occupancy levels, whereas increasingly curved shapes (i.e., those initially very steep or very shallow) will be of diminishing biological utility. To gauge the "usefulness" of any gradient shape, we take the distance between locations at which receptor occupancy falls from 2/3 to 1/3 of its maximum value and then normalize this number to $x_{max}/3$, the distance over which the equivalent fall occurs in a linear gradient. The resulting criterion, which we call η, can vary from 0 to 1, with the

highest values representing the most nearly linear gradients. In the present study, we use $\eta = 0.5$ as a (fairly generous) cutoff for biologically usefulness (see Figure 5C for examples). Figures published by Teleman and Cohen (2000) and Entchev et al. (2000) imply $\eta \approx 0.84$ for the Dpp gradient in the wing disc.

Modeling Random Nondiffusive Transport

A steady-state solution for random nondiffusive transport (equation 8 in Figure 2), in which $B = [LR]/R_{tot}$, and with the boundary condition that $B = 0$ at $x = x_{max}$, is $B = B_0\mathrm{Csch}(\delta)\mathrm{Sinh}(\delta(1 - x/x_{max}))$, where $\delta = \sqrt{(k_{deg}x_{max}^2/D^*)}$ and B_0 is the value of B at $x = 0$. From boundary equations, B_0 is found to be equal to $\nu/k_{deg}R_{tot}$. The transient solution for B may be expressed as

$$B = B_0\left((1 - e^{-k_{deg}t})(1 - x) - 2\sum_{n=1}^{\infty}\frac{\sin(n\,\pi\,\delta)\,(1 - e^{-k_{deg}t((\frac{n\pi}{\delta})^2+1)})}{n\,\pi\,((\frac{n\,\pi}{\delta})^2 + 1)}\right)$$

provided that ν, k_{on}, and k_{off} are sufficiently fast that [L] and [LR] equilibrate relatively rapidly at $x = 0$. To the extent they do not, the rate of formation of B will necessarily be slower than this expression predicts. Since we are concerned here only with the maximum rate at which nondiffusive transport can generate a steady-state gradient, this expression will suffice for our purposes.

From the steady state and transient solutions, it is straightforward to calculate the values of k_{deg} and D^*/x_{max}^2 that permit gradients to form rapidly enough (e.g., 60% of steady-state levels at $x = x_{max}/2$ by 7 hr) and are sufficiently linear to be biologically useful ($\eta = 0.5$).

Acknowledgments

We thank Kavita Arora, Ira Blitz, Ken Cho, and Larry Marsh for helpful discussions and reading of the manuscript. Simulations and analysis carried out with Richard L. S. Stein provided helpful initial insights. The work was supported by NIH grants HD038761 and NS26862.

Received: October 1, 2001
Revised: February 15, 2002

References

Baeg, G.H., and Perrimon, N. (2000). Functional binding of secreted molecules to heparan sulfate proteoglycans in *Drosophila*. Curr. Opin. Cell Biol. *12*, 575–580.

Berg, H.C. (1993). Random Walks in Biology, Second Edition (Princeton, New Jersey: Princeton University Press).

Bretscher, M.S. (1996). Expression and changing distribution of the human transferrin receptor in developing *Drosophila* oocytes and embryos. J. Cell Sci. *109*, 3113–3119.

Briscoe, J., and Ericson, J. (1999). The specification of neuronal identity by graded Sonic Hedgehog signalling. Semin. Cell Dev. Biol. *10*, 353–362.

Brummel, T.J., Twombly, V., Marques, G., Wrana, J.L., Newfeld, S.J., Attisano, L., Massague, J., O'Connor, M.B., and Gelbart, W.M. (1994). Characterization and relationship of Dpp receptors encoded by the saxophone and thick veins genes in *Drosophila*. Cell *78*, 251–261.

Cadigan, K.M., Fish, M.P., Rulifson, E.J., and Nusse, R. (1998). Wingless repression of *Drosophila* frizzled 2 expression shapes the Wingless morphogen gradient in the wing. Cell *93*, 767–777.

Capdevila, J., Pariente, F., Sampedro, J., Alonso, J.L., and Guerrero, I. (1994). Subcellular localization of the segment polarity protein patched suggests an interaction with the wingless reception complex in *Drosophila* embryos. Development *120*, 987–998.

Chen, M.S., Obar, R.A., Schroeder, C.C., Austin, T.W., Poodry, C.A., Wadsworth, S.C., and Vallee, R.B. (1991). Multiple forms of dynamin are encoded by *shibire*, a *Drosophila* gene involved in endocytosis. Nature *351*, 583–586.

Chuang, P.T., and Kornberg, T.B. (2000). On the range of hedgehog signaling. Curr. Opin. Genet. Dev. *10*, 515–522.

Cussler, E.L. (1997). Diffusion, Mass Transfer in Fluid Systems, Second Edition (Cambridge, UK: Cambridge University Press).

De Crescenzo, G., Grothe, S., Zwaagstra, J., Tsang, M., and O'Connor-McCourt, M.D. (2001). Real-time monitoring of the interactions of transforming growth factor-β (tgf-β) isoforms with latency-associated protein and the ectodomains of the tgf-β type II and III receptors reveals different kinetic models and stoichiometries of binding. J. Biol. Chem. *276*, 29632–29643.

Dyson, S., and Gurdon, J.B. (1998). The interpretation of position in a morphogen gradient as revealed by occupancy of activin receptors. Cell *93*, 557–568.

Eaton, S., Auvinen, P., Luo, L., Jan, Y.N., and Simons, K. (1995). CDC42 and Rac1 control different actin-dependent processes in the *Drosophila* wing disc epithelium. J. Cell Biol. *131*, 151–164.

Entchev, E.V., Schwabedissen, A., and Gonzalez-Gaitan, M. (2000). Gradient formation of the TGF-beta homolog Dpp. Cell *103*, 981–991.

Gonzalez, F., Swales, L., Bejsovec, A., Skaer, H., and Martinez Arias, A. (1991). Secretion and movement of wingless protein in the epidermis of the *Drosophila* embryo. Mech. Dev. *35*, 43–54.

González-Gaitan, M., and Jackle, H. (1999). The range of spalt-activating Dpp signalling is reduced in endocytosis- defective *Drosophila* wing discs. Mech. Dev. *87*, 143–151.

Greco, V., Hannus, M., and Eaton, S. (2001). Argosomes: a potential vehicle for the spread of morphogens through epithelia. Cell *106*, 633–645.

Groppe, J., Rumpel, K., Economides, A.N., Stahl, N., Sebald, W., and Affolter, M. (1998). Biochemical and biophysical characterization of refolded *Drosophila* DPP, a homolog of bone morphogenetic proteins 2 and 4. J. Biol. Chem. *273*, 29052–29065.

Gurdon, J.B., and Bourillot, P.Y. (2001). Morphogen gradient interpretation. Nature *413*, 797–803.

Gurdon, J.B., Dyson, S., and St Johnston, D. (1998). Cells' perception of position in a concentration gradient. Cell *95*, 159–162.

Hausen, P., and Riebesell, M. (1991). The Early Development of *Xenopus laevis* (Berlin: Springer Verlag).

Iwasaki, S., Tsuruoka, N., Hattori, A., Sato, M., Tsujimoto, M., and Kohno, M. (1995). Distribution and characterization of specific cellular binding proteins for bone morphogenetic protein-2. J. Biol. Chem. *270*, 5476–5482.

Jackson, S.M., Nakato, H., Sugiura, M., Jannuzi, A., Oakes, R., Kaluza, V., Golden, C., and Selleck, S.B. (1997). *dally*, a *Drosophila* glypican, controls cellular responses to the TGF-β-related morphogen, Dpp. Development *124*, 4113–4120.

Jortikka, L., Laitinen, M., Lindholm, T.S., and Marttinen, A. (1997). Internalization and intracellular processing of bone morphogenetic protein (BMP) in rat skeletal muscle myoblasts (L6). Cell. Signal. *9*, 47–51.

Keller, H.B. (1992). Numerical Methods for Two-Point Boundary-Value Problems (New York: Dover Publications).

Kerszberg, M., and Wolpert, L. (1998). Mechanisms for positional signalling by morphogen transport: a theoretical study. J. Theor. Biol. *191*, 103–114.

Koenig, J.H., and Ikeda, K. (1996). Synaptic vesicles have two distinct recycling pathways. J. Cell Biol. *135*, 797–808.

Lander, A.D. (1999). Seeking the functions of cell surface heparan sulphate proteoglycans. In Cell Surface Proteoglycans in Signalling and Development (Human Frontiers Science Program Workshop VI), A.D. Lander, H. Nakato, S. Selleck, J. Turnbull, and C. Coath, eds. (Strasbourg: HFSP), pp. 73–87.

Lauffenburger, D.A., and Linderman, J.J. (1993). Receptors. Models for Binding, Trafficking and Signaling (New York: Oxford University Press).

Lawrence, P.A. (2001). Wingless signalling: more about the Wingless morphogen. Curr. Biol. *11*, R638–639.

Lecuit, T., and Cohen, S.M. (1998). Dpp receptor levels contribute to shaping the Dpp morphogen gradient in the *Drosophila* wing imaginal disc. Development *125*, 4901–4907.

Leof, E.B. (2000). Growth factor receptor signalling: location, location, location. Trends Cell Biol. *10*, 343–348.

McDowell, N., and Gurdon, J.B. (1999). Activin as a morphogen in *Xenopus mesoderm* induction. Semin. Cell Dev. Biol. *10*, 311–317.

McDowell, N., Gurdon, J.B., and Grainger, D.J. (2001). Formation of a functional morphogen gradient by a passive process in tissue from the early *Xenopus* embryo. Int. J. Dev. Biol. *45*, 199–207.

Moline, M.M., Southern, C., and Bejsovec, A. (1999). Directionality of wingless protein transport influences epidermal patterning in the *Drosophila* embryo. Development *126*, 4375–4384.

Narayanan, R., and Ramaswami, M. (2001). Endocytosis in *Drosophila*: progress, possibilities, prognostications. Exp. Cell Res. *271*, 28–35.

Natsume, T., Tomita, S., Iemura, S., Kinto, N., Yamaguchi, A., and Ueno, N. (1997). Interaction between soluble type I receptor for bone morphogenetic protein and bone morphogenetic protein-4. J. Biol. Chem. *272*, 11535–11540.

Nellen, D., Burke, R., Struhl, G., and Basler, K. (1996). Direct and long-range action of a DPP morphogen gradient. Cell *85*, 357–368.

Neumann, C.J., and Cohen, S.M. (1997). Long-range action of Wingless organizes the dorsal-ventral axis of the *Drosophila* wing. Development *124*, 871–880.

Nicholson, C., and Sykova, E. (1998). Extracellular space structure revealed by diffusion analysis. Trends Neurosci. *21*, 207–215.

Pfeiffer, S., and Vincent, J.P. (1999). Signalling at a distance: transport of Wingless in the embryonic epidermis of Drosophila. Semin. Cell Dev. Biol. *10*, 303–309.

Poodry, C.A., and Schneiderman, H.A. (1970). The ultrastructure of the developing leg of *Drosophila melanogaster*. Wilhelm Roux' Arch. *166*, 1–44.

Rusakov, D.A., and Kullmann, D.M. (1998). Geometric and viscous components of the tortuosity of the extracellular space in the brain. Proc. Natl. Acad. Sci. USA *95*, 8975–8980.

Sainte-Marie, J., Vidal, M., Bette-Bobillo, P., Philippot, J.R., and Bienvenue, A. (1991). The influence of transferrin binding to L2C guinea pig leukemic lymphocytes on the endocytosis cycle kinetics of its receptor. Eur. J. Biochem. *201*, 295–302.

Scheufler, C., Sebald, W., and Hulsmeyer, M. (1999). Crystal structure of human bone morphogenetic protein-2 at 2.7 A resolution. J. Mol. Biol. *287*, 103–115.

Sheff, D.R., Daro, E.A., Hull, M., and Mellman, I. (1999). The receptor recycling pathway contains two distinct populations of early endosomes with different sorting functions. J. Cell Biol. *145*, 123–139.

Shitara, Y., Kato, Y., and Sugiyama, Y. (1998). Effect of brefeldin A and lysosomotropic reagents on intracellular trafficking of epidermal growth factor and transferring in Madin-Darby canine kidney epithelial cells. J. Controlled Release *55*, 35–43.

Strigini, M., and Cohen, S.M. (1997). A Hedgehog activity gradient contributes to AP axial patterning of the *Drosophila* wing. Development *124*, 4697–4705.

Strigini, M., and Cohen, S.M. (2000). Wingless gradient formation in the Drosophila wing. Curr. Biol. *10*, 293–300.

Strikwerda, J.C. (1989). Finite Difference Schemes and Partial Differential Equations (Pacific Grove, CA: Wadsworth & Brooks/Cole).

Tabata, T., and Kornberg, T.B. (1994). Hedgehog is a signaling protein with a key role in patterning *Drosophila* imaginal discs. Cell *76*, 89–102.

Teleman, A.A., and Cohen, S.M. (2000). Dpp gradient formation in the *Drosophila* wing imaginal disc. Cell *103*, 971–980.

The, I., Bellaiche, Y., and Perrimon, N. (1999). Hedgehog movement is regulated through tout velu-dependent synthesis of a heparan sulfate proteoglycan. Mol. Cell *4*, 633–639.

Tickle, C. (1999). Morphogen gradients in vertebrate limb development. Semin. Cell Dev. Biol. *10*, 345–351.

van der Bliek, A.M., and Meyerowitz, E.M. (1991). Dynamin-like protein encoded by the *Drosophila* shibire gene associated with vesicular traffic. Nature *351*, 411–414.

Zecca, M., Basler, K., and Struhl, G. (1996). Direct and long-range action of a wingless morphogen gradient. Cell *87*, 833–844.

Zeng, X., Goetz, J.A., Suber, L.M., Scott, W.J., Jr., Schreiner, C.M., and Robbins, D.J. (2001). A freely diffusible form of Sonic hedgehog mediates long-range signalling. Nature *411*, 716–720.